Isolation, growth, and nitrogen fixation rates of the *Hemiaulus-Richelia* (diatom-cyanobacterium) symbiosis in culture

Amy E. Pyle[1], Allison M. Johnson[2] and Tracy A. Villareal[1]

[1] Department of Marine Science and Marine Science Institute, The University of Texas at Austin, Port Aransas, TX, USA
[2] St. Olaf College, Northfield, MN, USA

ABSTRACT

Nitrogen fixers (diazotrophs) are often an important nitrogen source to phytoplankton nutrient budgets in N-limited marine environments. Diazotrophic symbioses between cyanobacteria and diatoms can dominate nitrogen-fixation regionally, particularly in major river plumes and in open ocean mesoscale blooms. This study reports the successful isolation and growth in monocultures of multiple strains of a diatom-cyanobacteria symbiosis from the Gulf of Mexico using a modified artificial seawater medium. We document the influence of light and nutrients on nitrogen fixation and growth rates of the host diatom *Hemiaulus hauckii* Grunow together with its diazotrophic endosymbiont *Richelia intracellularis* Schmidt, as well as less complete results on the *Hemiaulus membranaceus-R. intracellularis* symbiosis. The symbioses rates reported here are for the joint diatom-cyanobacteria unit. Symbiont diazotrophy was sufficient to support both the host diatom and cyanobacteria symbionts, and the entire symbiosis replicated and grew without added nitrogen. Maximum growth rates of multiple strains of *H. hauckii* symbioses in N-free medium with N_2 as the sole N source were 0.74–0.93 div d^{-1}. Growth rates followed light saturation kinetics in *H. hauckii* symbioses with a growth compensation light intensity (E_C) of 7–16 µmol $m^{-2}s^{-1}$and saturation light level (E_K) of 84–110 µmol $m^{-2}s^{-1}$. Nitrogen fixation rates by the symbiont while within the host followed a diel pattern where rates increased from near-zero in the scotophase to a maximum 4–6 h into the photophase. At the onset of the scotophase, nitrogen-fixation rates declined over several hours to near-zero values. Nitrogen fixation also exhibited light saturation kinetics. Maximum N_2 fixation rates (84 fmol N_2 heterocyst$^{-1}h^{-1}$) in low light adapted cultures (50 µmol $m^{-2}s^{-}1$) were approximately 40–50% of rates (144–154 fmol N_2 heterocyst$^{-1}h^{-1}$) in high light (150 and 200 µmol $m^{-2}s^{-1}$) adapted cultures. Maximum laboratory N_2 fixation rates were ~6 to 8-fold higher than literature-derived field rates of the *H. hauckii* symbiosis. In contrast to published results on the *Rhizosolenia-Richelia* symbiosis, the *H. hauckii* symbiosis did not use nitrate when added, although ammonium was consumed by the *H. hauckii* symbiosis. Symbiont-free host cell cultures could not be established; however, a symbiont-free *H. hauckii* strain was isolated directly from the field and grown on a nitrate-based medium that would not support DDA growth. Our observations together with literature reports raise the

Submitted 28 April 2020
Accepted 16 September 2020
Published 8 October 2020

Corresponding author
Tracy A. Villareal,
tracyv@austin.utexas.edu

Academic editor
Konstantinos Kormas

Additional Information and Declarations can be found on page 19

DOI **10.7717/peerj.10115**

possibility that the asymbiotic *H. hauckii* are lines distinct from an obligately symbiotic *H. hauckii* line. While brief descriptions of successful culture isolation have been published, this report provides the first detailed description of the approaches, handling, and methodologies used for successful culture of this marine symbiosis. These techniques should permit a more widespread laboratory availability of these important marine symbioses.

Subjects Ecology, Marine Biology, Microbiology, Biological Oceanography
Keywords Symbiosis, Diazotrophy, Diatom, Cyanobacteria, Culture, Marine, Hemiaulus, Richelia, Nitrogen-fixation, DDA

INTRODUCTION

The phytoplankton flora of the open sea is a diverse assemblage of prokaryotic and eukaryotic cells that span a size range of ~1 to 2,000+ µm in diameter. Nitrogen is often a limiting nutrient in the open sea, and planktonic nitrogen fixation (diazotrophy) occurs in tropical, subtropical systems and high latitude systems (*Zehr, 2011*; *Harding et al., 2018*). However, nitrogen fixation can occur in a wide variety of deep-sea and benthic habitats not traditionally associated with nitrogen-limitation (*Zehr & Capone, 2020*). Diazotrophy occurs only in prokaryotic cells, but a variety of symbiotic associations between diazotrophic prokaryotes and host eukaryotes are known (*Foster, Carpenter & Bergman, 2006*; *Foster & O'Mullan, 2008*; *Taylor, 1982*; *Villareal, 1992*; *Zehr & Capone, 2020*) and cover the range from obligate symbioses to loosely associated consorts (*Caputo, Nylander & Foster, 2019*; *Carpenter, 2002*; *Foster, Carpenter & Bergman, 2006*; *Foster & O'Mullan, 2008*). Of these, diatom-diazotroph associations (DDAs) are the most visible with records dating back to the early 20th century (*Karsten, 1905*).

Two types of marine diatom-cyanobacteria symbioses are known: diatoms in the genera *Neostreptotheca* and *Climacodium* that host coccoid cyanobacteria (*Carpenter & Janson, 2000*; *Hallegraeff & Jeffrey, 1984*), and diatoms that host filamentous, heterocyst-forming cyanobacteria of the genera *Richelia* and *Calothrix*. Little is known about the characteristics of the coccoid symbionts in diatoms, although the *Climacodium* symbiont is a diazotrophic *Crocosphaera* sp. (*Foster et al., 2011*). DDA symbioses involving heterocystous, diazotrophic cyanobacteria are abundant in both open ocean systems (*Dore et al., 2008*; *Villareal et al., 2011*; *Wilson et al., 2008*) and at intermediate salinities within the Amazon (*Foster et al., 2007*), Mekong (*Grosse et al., 2009*) and Congo River plumes (*Foster, Subramaniam & Zehr, 2009*). These marine regions differ greatly in their characteristics, suggesting either a great plasticity in physiological responses to environmental variables or undocumented differentiation within these symbioses. Symbiont integration with the hosts varies as well. In the *Rhizosolenia-Richelia* DDA symbiosis, the symbiont is located in the periplasmic space between the frustule and plasmalemma and has limited contact with the external environment (*Janson et al., 1999*; *Villareal, 1989*). The *Hemiaulus-Richelia* DDA symbiont is appressed to the nucleus and truly intracellular (*Caputo, Nylander & Foster, 2019*), consistent with its reduced

genome (*Hilton et al., 2013*). The *Chaetoceros-Calothrix* DDA symbiont is completely extracellular to the host diatom (*Foster, Goebel & Zehr, 2010*).

Despite their ubiquitous occurrence in tropical seas, the *Hemiaulus-Richelia* symbiosis was largely overlooked until epifluorescence microscopy revealed the cryptic *Richelia* symbiont (*Heinbokel, 1986*) and N_2 fixation was documented in individually picked chains of the symbiosis (*Villareal, 1991*). In addition to providing fixed N to the pelagic community, diatom-cyanobacteria symbioses play an important role in the nitrogen and carbon cycles of oceanic systems by virtue of their potential to sequester carbon to the deep sea via aggregation and sinking (*Karl et al., 2012*; *Subramaniam et al., 2008*). In the currency of oceanic nitrogen cycling, nitrogen derived from photosynthetic nitrogen fixation is generally balanced by a concurrent removal of atmospheric CO_2 (*Eppley & Peterson, 1979*). Thus, sinking material fueled by phototrophic diazotrophy represents a net removal of CO_2, and is a quantitatively important process in the transport of carbon to depth. DDAs, and particularly *Hemiaulus* symbioses, are of particular oceanographic significance. *Hemiaulus-Richelia* symbioses bloom at ~10^3 cells L^{-1} frequently at the Hawai'i Ocean Time-series HOT (*Dore et al., 2008*; *Fong et al., 2008*; *Scharek et al., 1999*; *White, Spitz & Letelier, 2007*). At this location, they are the likely source of the summer export pulse that provides 20% of the annual carbon flux to 4,000 m in a 4–6-week window (*Karl et al., 2012*) and are regularly found on sinking particles (*Farnelid et al., 2019*). Subtropical front blooms at ~28–30°N in the Pacific (*Venrick, 1974*; *Villareal et al., 2012*; *Wilson, Villareal & Bogard, 2004*; *Wilson et al., 2008*) and in waters west and north of HI (*Brzezinski, Villareal & Lipschultz, 1998*; *Villareal et al., 2011*) suggest a basin scale significance. In the southwest Atlantic Ocean, *Hemiaulus hauckii-Richelia* blooms cover 10^5+ km^2 and sequester 1.7 Tmol of carbon annually (*Carpenter et al., 1999*; *Subramaniam et al., 2008*) and CO_2 drawdown effects can extend to 10^6 km^2 (*Cooley et al., 2007*). The large size, chain-formation, and tendency to aggregate (*Scharek et al., 1999*; *Villareal et al., 2011*) in the host *Hemiaulus* lead to an efficient export mechanism (*Yeung et al., 2012*) for both N and C.

Culture studies on the growth and physiological characteristics of these symbioses are limited. The external symbiont *Calothrix rhizosoleniae* has been cultured without its host (*Foster, Goebel & Zehr, 2010*) in both natural and artificial seawater medium. Cultures of the *Rhizosolenia-Richelia* symbiosis using amended seawater have been reported in the literature with growth rates up to 0.8 div d^{-1} in fixed N-free medium (*Villareal, 1990*). In the *Rhizosolenia-Richelia* DDA, host and symbiont growth can be independent and symbiont-free host cells occur (but have reduced growth rates) even when no fixed N is present, possibly through use of N excreted by *Richelia* into the medium. Addition of nitrate rapidly results in the loss of symbionts as asymbiotic *Rhizosolenia* uses the added nitrate, increases its growth rate, and out-competes symbiotic *Rhizosolenia-Richelia* (*Villareal, 1989*, *1990*). Nitrogen fixation follows typical light saturation kinetics and can provide the entire N needs of the symbiosis (*Villareal, 1990*). Although oceanographically more significant than other *Rhizosolenia-Richelia* DDA (*Heinbokel, 1986*; *Subramaniam et al., 2008*; *Villareal, 1992*), there are no published culture-based data for the *Hemiaulus-Richelia* symbiosis.

Using nano-SIMS on field samples, *Foster et al. (2011)* were able to document the transport of recently fixed N from the symbiont *Richelia* to the host *Hemiaulus* in sufficient quantities to support growth; however, it is not known whether *Hemiaulus-Richelia* can grow exclusively on diazotrophically fixed N. Regardless, the symbiont is clearly advantageous to the host since, where examined, 80–100% of the *Hemiaulus* contain the symbiont (*Bar-Zeev et al., 2008*; *Heinbokel, 1986*; *Villareal, 1991*, *1994*) and 85–100% of the total phytoplankton N needs in the Amazon River plume can be met by *Hemiaulus* DDA diazotrophy (*Carpenter et al., 1999*; *Weber et al., 2017*). The symbiosis is not obligate for the host *Rhizosolenia* in DDA cultures (*Villareal, 1990*) and the field evidence suggests this may also be true for the host *Hemiaulus* (*Heinbokel, 1986*; *Kimor, Reid & Jordan, 1978*). This latter hypothesis has not been tested due to the difficulty in growing the *Hemiaulus-Richelia* host-symbiont pair in vitro.

In this article, we report the successful isolation of two species of the *Hemiaulus-Richelia* symbiosis into culture and expand on the brief culturing description reported in *Schouten et al. (2013)*. Using primarily *H. hauckii-Richelia* DDA strains, we document light-dependent growth rates, diel cycles of N_2 fixation, growth rate response to various forms of added nitrogen, and N_2 fixation rates. These parameters are essential to supporting modeling of DDA bloom formation and fate (*Follett et al., 2018*; *Stukel et al., 2014*). In addition, key differences between the *Hemiaulus* and *Rhizosolenia* DDAs are noted.

METHODS AND MATERIALS

All culturing was conducted at the University of Texas Marine Science Institute (UTMSI) in Port Aransas, Texas. *Hemiaulus* strains containing symbionts were isolated by micropipette (*Andersen & Kawachi, 2005*) from the Port Aransas ship channel (27° 57′ 17.56″ N, 90° 03″ 00.48″ W) using material from either net tows (20–35 µm mesh nets, 1–3 min tows in the incoming tide) or whole water samples (incoming tide). The net tow sample was collected from a platform under a pier laboratory that both shaded the sample from direct sun the entire time as well as facilitating numerous short tows resulting in dilute samples. Both initial isolations and subsequent cultures of symbiont containing *Hemiaulus* were maintained in sterile filtered, fixed N-free YBCII media with L1 trace metal/EDTA additions (*Ohki, Zehr & Fujita, 1992*; *Chen, Zehr & Mellon, 1996*; *Guillard & Hargraves, 1993*), and final concentrations of 1 µm sodium glycerophosphate ($C_3H_7Na_2O_6P$), 2.6 µm sodium dihydrogen phosphate monohydrate ($NaH_2PO_4 \cdot H_2O$) and 35.7 µm sodium metasilicate ($Na_2SiO_3 \cdot 9H_2O$). Throughout the text, N-free or fixed N-free medium will refer to culture medium that has no added organic or inorganic N, recognizing that dissolved N_2 will be abundant as an N source for diazotrophs. Sterile filtered medium and seawater were generated using commercially available sterile tissue culture towers and reservoirs (0.22 µm pore size filters). Sterile filtration units were rinsed with ~50 ml of medium prior to use for culture medium. Both nylon and methyl cellulose 0.22 µm pore size filters were used with no apparent difference in results. All chemicals were reagent grade or better. The modified YBCII medium was checked with a hand-held refractometer before each use and adjusted to a salinity of 35 as

needed using 18 megaohm deionized water. Autoclaved tubes were rinsed with sterile filtered medium and then the tube filled with 15–20 mL of medium. This rinsing step was used for all flasks and tubes used for culturing.

Isolations were performed within 5–10 min of collection. Using a stereomicroscope, multiple *Hemiaulus* chains were rapidly isolated from the net tow material using hand-held borosilicate pipets drawn to a fine diameter in a gas flame. In our work, the drawn-out pipets were attached with tubing to a cotton-plugged mouthpiece (to prevent seawater aspiration) of fire-polished glass tubing. Mouth pipetting was used to carefully draw or expel the chain. If mouth pipetting is unacceptable, any form of fine control would provide adequate results. Multiple *Hemiaulus* chains were isolated into one well of a glass depression well plate (16 depressions) containing ~2 ml of medium per depression. Individual chains were then rinsed via serial transfer into other wells containing sterile medium. Extensive rinsing (5–6 rinses) of a single chain before isolating the next chain was much less successful than only 2–3 rinses before placing the chain into a tube of medium. When isolated directly into the N-deplete modified YBCII medium, contaminant growth was minimal even with only 1–2 rinses. These techniques resulted in symbiosis isolation free of other eukaryotes or cyanobacteria in ~30–40% of the attempts. Preliminary experiments used *H. hauckii* strain #9 isolated during Spring 2010. Subsequent *H. hauckii* experiments used isolates established during Fall 2010 (strain #22) and Fall 2011 (strain #83, #91, and #92). *Hemiaulus membranaceus* strain #82 was isolated in the Fall 2011. In all subsequent text, a strain designation indicates a culture of a host diatom containing one or more symbionts. While *Hemiaulus hauckii* strain #91 was used for most of the experiments, a single strain for the entire suite of experiments was not possible due to loss of the strain or the periodic loss of vitality noted in the results. Strains used are identified in the text and in Table S1.

The *Hemiaulus* DDA could be isolated for short-term growth into MET-44 (*Schöne & Schöne, 1982*) nutrient-amended (no added nitrate) sterile filtered seawater (0.22 µm filter equipped commercial sterile filtration units) collected at the isolation point. However, the *Hemiaulus-Richelia* symbioses required re-isolation from this MET-44 medium into the modified YBCII medium for successful maintenance >2–3 weeks. After isolation, cells were placed in a 25 °C incubator under cool white fluorescent illumination of 150–250 µmol m^{-2} s^{-1} on a 12:12 Light:Dark (L:D) cycle. All cultures were grown as batch cultures. Cultures had a high rate of sudden decline and death when kept in medium longer than 7–10 days and careful attention was required to transfer the cultures to new medium within this time frame. Experiments were initiated within 6 months of culture isolation; cultures failed to make auxospores and were eventually lost after approximately 1–2 years in culture. No attempt was made to culture axenically; bacteria were rarely visible in the cultures under phase contrast or differential interference contrast optics until senescence when cell mortality was substantial. *The H. hauckii* DDA was the primary experimental tool. *Hemiaulus membranaceus* DDA cultures were examined for general characteristics but were not the subject of intensive experimentation. In March 2017, *Hemiaulus* chains were observed in the Port Aransas ship channel from the Imaging Flow Cytobot data stream (*Campbell et al., 2010*, *2017*). Examination of net tow material noted

numerous asymbiotic *H. hauckii* chains and no symbiotic cells. Asymbiotic chains of *Hemiaulus hauckii* were isolated into N-replete (40 µm NO_3^-) MET-44 amended sterile filtered seawater as noted above. Unless otherwise noted, all experiments were conducted using modifies YBCII medium with no added nitrogen. Dissolved N_2 was the only available nitrogen source.

Analytical methods

Cells were counted using a S52 Sedgewick-Rafter chamber on an Olympus BX51 epifluorescence microscope. Excitation/emission wavelengths for the epifluorescent filters used in counts and photography were 450 nm/680 nm (chlorophyll *a*), and 490 nm/565 nm (phycoerythrin). Both host cells and symbiont trichomes/heterocysts were enumerated. Percent symbiosis was calculated as the number of diatoms containing one or more *Richelia* trichomes divided by the total number of potential host cells. Growth rates (reported as div d^{-1}) were calculated using daily counts as the slope of the log of cell number over the change in time (*Guillard, 1973*) with the 95% confidence interval around the slope of the line calculated in Microsoft Excel.

Acetylene reduction assays (ARA) were performed as described in *Capone (1993)* corrected for ethylene solubility as described by *Breitbarth et al. (2004)* and assuming a mol ethylene reduced per mol N_2 conversion ratio of 4:1 (*Jensen & Cox, 1983* as modified by *Capone, 1993*). An SRI 8610C gas chromatograph (SRI Instruments, Torrance, CA, USA) equipped with a 30 cm silica gel column was used to quantify ethylene using a commercially prepared standard (GASCO Safeware Precision Gas Mixture, 10 and 100 ppm). Manufacturer-provided software (PeakSimple Chromatography Software) performed peak integrations. Standards were run prior to each day's run and at several points during the experiment. For each assay, 15 ml of culture sample was added to an acid-washed 25 ml incubation vial fitted with a gray chlorobutyl rubber serum stopper and crimped aluminum seals leaving 10 ml of headspace. Sterile-filtered medium was used as a control. A separate aliquot was retained for cell counts. One ml of acetylene generated from calcium carbide (*Capone, 1993*) was introduced, gently swirled for 15–30 s to equilibrate while minimizing contact between the serum stopper and the culture, then 100 µL of the vial headspace injected with a Hamilton gas-tight syringe and injected into the GC. Each injection required 5–7 min after an injection to return to baseline.

Chlorophyll *a* was determined on methanol-extracted (24 h, –20 °C) samples (10–25 ml aliquot) collected on 0.4 µm pore size polycarbonate filters using a non-acidification method (*Welschmeyer, 1994*). Initial tests indicated the filters used did not leach fluorescent compounds in the methanol. When chl *a* $cell^{-1}$ is referred to, it always includes both symbiont and host chl *a*. Sample fluorescence was read on a TD-700 Fluorometer (Turner Designs, Fresno, CA, USA).

For nutrients, a 25 mm, 0.22 µm pore-size membrane cellulose ester Millipore filter mounted on a syringe was rinsed with 5 ml of sample, filtrate discarded, and ten ml of sample medium was filtered and frozen. A SEAL Analytical QuAAtro autoanalyzer was used to determine dissolved inorganic phosphate (DIP), nitrate +nitrite (N + N), ammonium (NH_4^+), and silicate (SiO_4^{-2}) concentrations using the manufacturer's

recommended chemistries. The chemistries are similar to automated analyses published in *Grasshoff, Kremling & Ehrhardt (1999)* with changes in reagent concentration and wetting agents specific to the manifold chemistries. Detection limits were ~0.05 µm for N + N, NH_4^+ and P, and ~0.5 µm for Si.

Growth-rate and N_2 fixation versus irradiance experiments

Hemiaulus hauckii symbiosis strains #9 and #91 were used for the irradiance-rate experiments. Initial experiments (Strain #9) used two light levels and are included for comparison. Detailed growth rates and N_2 fixation rates were measured in separate experiments using 7–8 different light levels (photosynthetic photon flux density) ranging from 15 to 600 µmol m^{-2} s^{-1} measured by a QSP-170B irradiance meter (Biospherical Instruments; Table S1). For growth rates, cultures were grown at the 7 experimental light levels for 7 days and remained at the assigned light level through the duration of the experiments. Symbiosis growth is used throughout this paper to refer to increases in host diatom numbers containing at least one symbiont. For N_2 fixation, strains were adapted to either 50, 150, or 200 (high light HL) µmol m^{-2} s^{-1} at 25 °C and a salinity of 35 under cool white fluorescent lighting for 7 days prior to the acetylene reduction assay. Each adaptation level was then exposed to 7–8 light levels for acetylene reduction assay.

Diel pattern of N_2 fixation

Hemiaulus hauckii strains #22 and #92, and *H. membranaceus* strain #82 were used for the diel study (12:12 L:D cycles at 200 µmol $m^{-2}s^{-1}$) examining the daily rhythm of N_2 fixation on culture medium with no added N. Initial experiments on *H. hauckii* strain #22 utilized a set of 6 discrete time points between 06:00 and 21:00. Each incubation lasted 4 h with initial and final measurements taken in triplicate. Rates were normalized to heterocysts and used the center point of the 4 h incubation period as the time stamp. Subsequent experiments on *H. hauckii* strain #92 and *H. membranaceus* strain #82 utilized a high frequency time series approach in order to resolve changes occurring on an hourly basis or less. This approach used a series of individual measurements taken from a single vial over a period of up to ~12 h and was utilized for two reasons. First, individual assays injections required 5–7 min to return to baseline. Triplicate measurements therefore required 15–21 min during which ethylene production was occurring at measurable rates, could not be consideration true replication of the ethylene measurement. Averages of these triplicates would be unable to resolve rate changes on short time scales. The second reason for this approach was to minimize handling, agitation, and light/temperature variation of the samples. Six (*H. hauckii*) or 8 (*H. membranaceus*) paired vials were started at various time points in the diel cycle to permit overlap. Individual time series can be identified from the labeling in Table S1. Vials were sampled sequentially (1a, 1b, 2a, 2b, 3a, 3b, then repeated) yielding approximately 1–1.5 h between successive sampling of a single vial. The difference between successive measurements (ethylene per heterocyst) was normalized to the time difference between the two successive points (~1 to 1.5 h) and expressed as a rate (ethylene $heterocyst^{-1}$ $time^{-1}$). Eighty-nine (*H. hauckii)* and 78 (*H. membranaceus)* separate measurements were plotted against time using a 5-point

running average (center point plus two on either side) to smooth the data. Rates from different vial series overlapped in time, thus the 5-point average has rates from independent time series. Standard deviation was calculated on this 5-point series recognizing this is not a statistically useful value but only a metric for the noise in the data. Experimental cultures were adapted to at 25 °C under 200 µmol m^{-2} s^{-1} illumination (cool-white fluorescence bulbs) on 12:12 LD cycle. Experimental vials were incubated under these same conditions. Samples during the scotophase were collected/returned to the incubator in a darkened container and shielded from the dimmed laboratory lights during the assay.

Nutrient addition experiments

Nitrogen source experiments addressed the effect of various inorganic N sources on symbiosis growth and N_2 fixation. In these experiments, *H. hauckii* strain # 83 was transferred to three 2 L autoclaved glass Erlenmeyer flasks containing the maintenance medium listed above amended with one of the following nitrogen sources: no added nitrogen (control), added nitrate (40 µm) or added ammonium (10 µm). Samples were maintained at 25 °C and a salinity of 35. Reduced ammonium concentrations were used to avoid toxicity effects; the nitrate concentration duplicated work on the *Rhizosolenia-Richelia* symbiosis (*Villareal, 1989*). Nutrient concentrations and cell abundance were sampled 10 times throughout the duration of the 20-day experiment. Nutrient analyses and cell counts were done in duplicate.

Curve-fitting and statistics

Light-dependent growth was fit to the Jassby-Platt hyperbolic tangent function (*Jassby & Platt, 1976*) with a y-intercept term to permit calculation of compensation light intensity. The y-intercept term was omitted for the N_2 fixation rates vs. irradiance curves due to time-dependent decline in dark N_2 fixation that became evident in the diel measurements. When not omitted, the time-dependent decline in dark N_2 fixation noted in the diel experiment at the beginning of the scotophase resulted in a highly variable initial slope as well as a significant y-intercept (dark fixation rate) that was not consistent with the longer term rates after several hours in darkness. Delta Graph (Red Rocks Software, Las Vegas, NV, USA) was used for graphics as well as curve fitting of the growth and N_2-irradiance curves. *T*-tests were performed using the data analysis package in Microsoft Excel. Confidence intervals or standard deviations (noted in text) were calculated using Microsoft Excel software. Data from all figures are found in Table S1.

RESULTS

Hemiaulus hauckii and *Hemiaulus membranaceus* with their symbiont *Richelia intracellularis* were successfully isolated multiple times. We found it was essential to remove the *Hemiaulus* from the net tow sample as quickly as possible (3–5 min after completion of the tow). Successful culturing resulted in rapidly growing chains of *Hemiaulus* reaching over 80 cells in length (Fig. 1). Multiple symbionts (usually 1–2, but never more than 4) were evident in the cells. Cultures were sensitive to handling, and

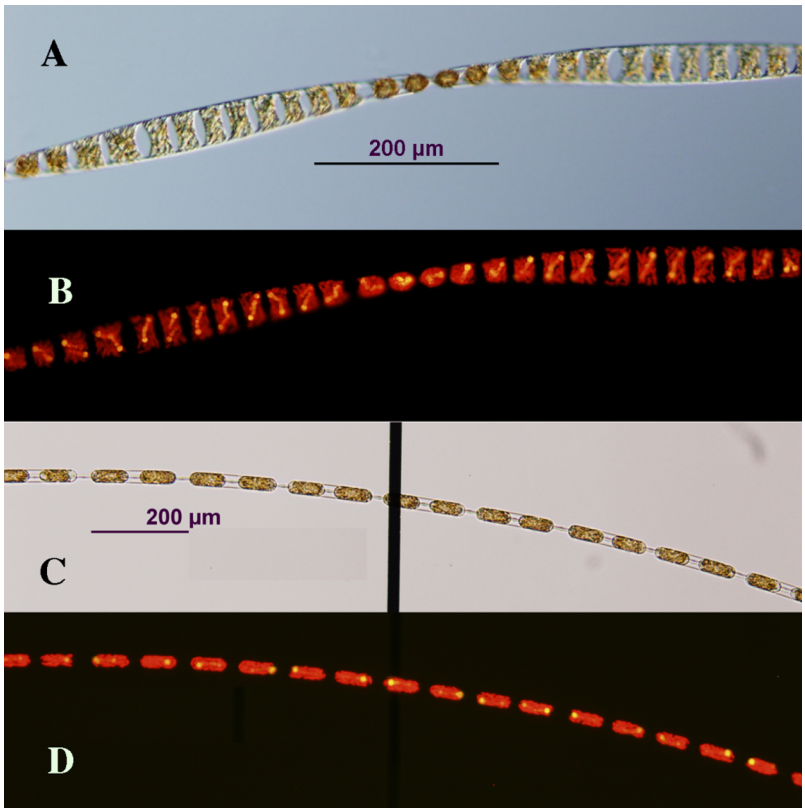

Figure 1 Photomicrographs of *Hemiaulus membranaceus* (A and B) and *H. hauckii* (C and D) symbioses cultured in this study. Images are paired photomicrographs of transmitted light micrographs (A and C) and light micrographs under epifluorescence (see "Methods") (B and D), and were taken from samples in a Sedgewick Rafter counting cell to minimize breakage of long chains. The vertical black bar in (C) is a marking from the Sedgewick Rafter cell. It lies under the chain; hence. it does not obscure details illuminated by epifluorescence in (D). Scale bar = 200 µm for all images. Image credit: A.E. Pyle. Full-size DOI: 10.7717/peerj.10115/fig-1

swirling tubes to re-suspend chains resulted in chain breakage and decreased growth rates. Growth in undisturbed large volume containers (10 L+) resulted in complex aggregate formation. Strains were difficult to ship, and only one attempt out of approximately 15 resulted in successful establishment in another facility. A single auxospore-like structure was observed, but no cell diameter increases were observed in any of the cultures.

Hemiaulus hauckii strains used in this study ranged from 12 to 17.5 µm (up to 30 µm observed) in diameter (pervalvar axis presented in broad girdle view) with a total cell volume range of 7,012–23,574 μm^3. *H. membranaceus* cells were not measured. Since auxosporulation did not occur, the strains gradually decreased in diameter over a period of 1–2 years and eventually died out. Individual strains exhibited periods (weeks/months) of healthy growth (0.5–0.9 div d^{-1}) with little care required. This growth pattern was interspersed with intervals (days/weeks) of low growth rates that required substantial attention and multiple backups to prevent loss of the culture. These cyclic patterns were not linked to batches of culture medium or glassware. While not enumerated, bacteria were

rarely evident in light microscopy but certainly present since the cultures were not axenic. Reasons for the observed growth pattern variability remain unknown.

Individual symbiosis strains were routinely maintained in modified YBC-II medium with no added nitrogen. High densities of *Hemiaulus* and its symbionts were possible with no N added to the synthetic seawater medium (residual combined inorganic N < 0.1 µm). Maximum cell counts of the host *H. hauckii* reached ~10,000 cells mL^{-1} with a maximum chl *a* concentration of 71 µg L^{-1}. Typical cell and chl *a* dynamics are shown in Fig. 2. High light (200 µmol m^{-2} s^{-1}) chl *a* concentration reached a maximum approximately 3.5 times greater than the low light (50 µmol m^{-2} s^{-1}) concentrations, although chl *a* per symbiosis (combined host and symbiont; multiple strains) remained approximately equal over time. In both light conditions, chl *a* per symbiosis was maximal (~4 to 5 pg chl *a* $symbiosis^{-1}$) in early exponential growth and declined over time to ~2 to 3 pg chl *a* $symbiosis^{-1}$. Extensive chain formation resulted in a high degree of variation in measurements.

Growth rates of *H. hauckii* in N-deplete medium (Fig. 3) followed light saturation kinetics with host and symbiont growth rates highly correlated ($r^2 = 0.98$, $p = 0.05$, *t*-test). Photoinhibition was not observed at the maximum light level used (500 µmol m^{-2} s^{-1}). A modified Jassby-Platt curve fit (Article S1) yielded a realized maximum growth rate µ of 0.74–0.93 div d^{-1} in replicated experiments (Fig. 3; Table 1). Light-saturated growth occurred with light saturation (E_k) occurring at 84–110 µmol m^{-2} s^{-1} and an initial slope (α) of 0.009 div d^{-1}(µmol m^{-2} s^{-1})$^{-1}$ in both irradiance curves. Compensation light intensity (E_c) calculated from the y-intercept and α varied from 7 to 16 µmol m^{-2} s^{-1}.

Nitrogen fixation rates estimated by acetylene reduction were tightly linked to the light: dark cycle (Fig. 4). The 5-point running average was necessary to smooth the variable point-to-point time series rates into a general diel curve. Two separate experimental treatments (the 4-h incubations and the 5-point averaging series) indicated the maximum acetylene reduction rate in both *H. hauckii* and *H. membranaceus* DDA occurred approximately 4 h into the photophase (12:12 photoperiod) with a broader maximum acetylene reduction rate extending for 4–6 h. Acetylene reduction declined over several hours at photophase end to low (1–10% maximum values) but still measurable rates during the scotophase in both *H. hauckii* (Fig. 4A) and *H. membranaceus* (Fig. 4B) DDAs. Unlike the 4-h discrete incubation diurnal pattern seen in Strain #22, *H. hauckii* strain #92 rates maintained high values until the end of the photophase (Fig. 4A). *Hemiaulus membranaceus* DDA rates were more symmetrically distributed around the middle of the photoperiod (Fig. 4B). In both data sets, the rates reached a maximum in the range of 45–55 fmol N_2 $heterocyst^{-1}$ h^{-1}.

Nitrogen fixation-irradiance rates followed a light saturation curve (Fig. 5) fit to the hyperbolic tangent function. At the 150 and 200 µmol m^{-2} s^{-1} adaptation level (r^2=0.95 and 0.97, respectively), the curve-fit maximum N_2-fixation rates was 155 and 144 fmol N_2 $heterocyst^{-1}$ h^{-1}, respectively. The maximum rates (light-saturated) at 150 and 200 µmol m^{-2} s^{-1} adaptation level were significantly ($p < 0.01$, *t*-test) greater than the maximum (light-saturated) rate (86 fmol N_2 $heterocyst^{-1}$ $h^{-1)}$ noted in cultures adapted to 50 µmol m^{-2} s^{-1}. The initial slope (light limited portion) of the N_2 fixation curve was

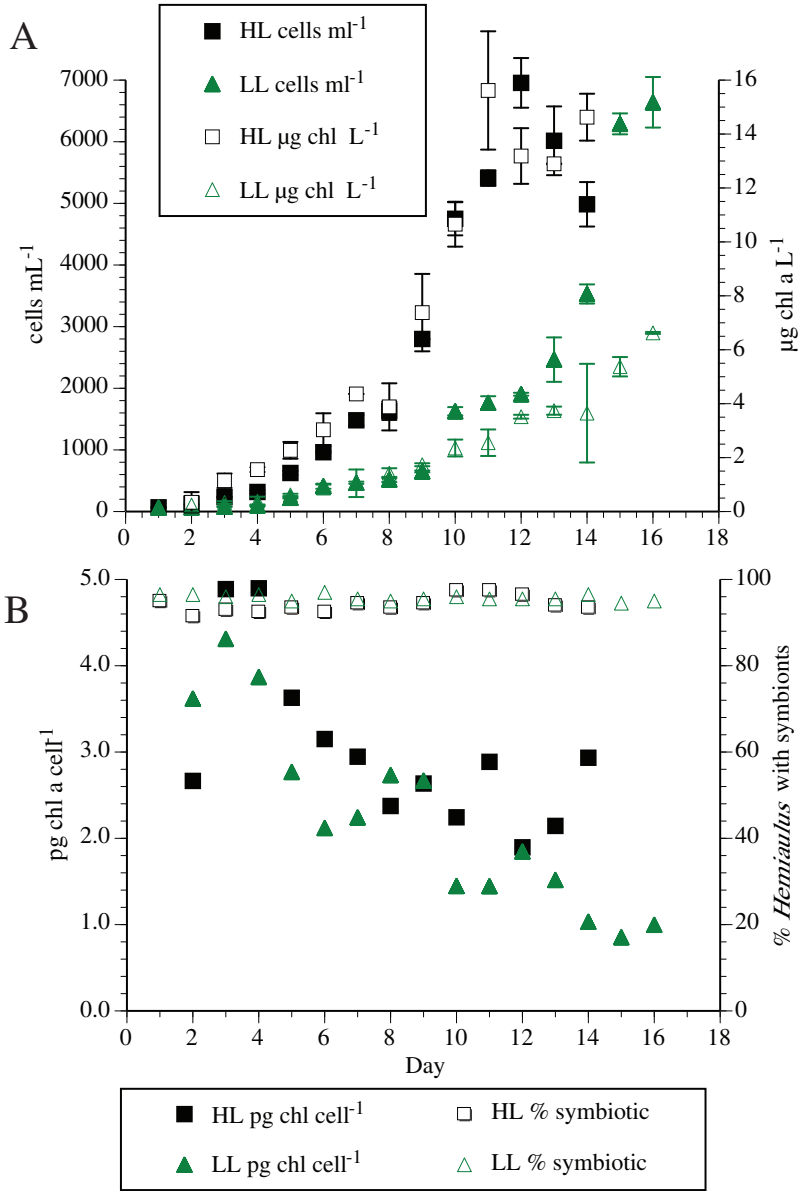

Figure 2 Typical *Hemiaulus hauckii* growth curve at two irradiance levels in modified YBC-II medium with no added nitrogen using strain #91. (A) Cell abundance and bulk chlorophyll *a* concentration. (B) Chlorophyll *a* content per host cell (sum of host and symbiont chl *a*) and symbiont presence in hosts. High light (HL: 200 µmol m^{-2} s^{-1}); Low light (LL: 50 µmol m^{-2} s^{-1}). Values are means of duplicates ± standard deviation. Full-size DOI: 10.7717/peerj.10115/fig-2

approximately 75% higher in the 50 µmol m^{-2} s^{-1} adapted culture than the 150 and 200 µmol m^{-2} s^{-1} adaptation level.

Preliminary experiments in 2010 found that *H. hauckii* strain #9 did not utilize nitrate (Table S2). Subsequent replication experiments found that 40 µm nitrate was not used by a different *H. hauckii* symbiosis strain (#83) in experiments conducted 1 year later (Fig. 6). Ten µM added ammonium declined to ~0.4 µm in 13 days and then remained constant thereafter (Fig. 6). *Hemiaulus hauckii* strain #83 drew down P and Si under all the

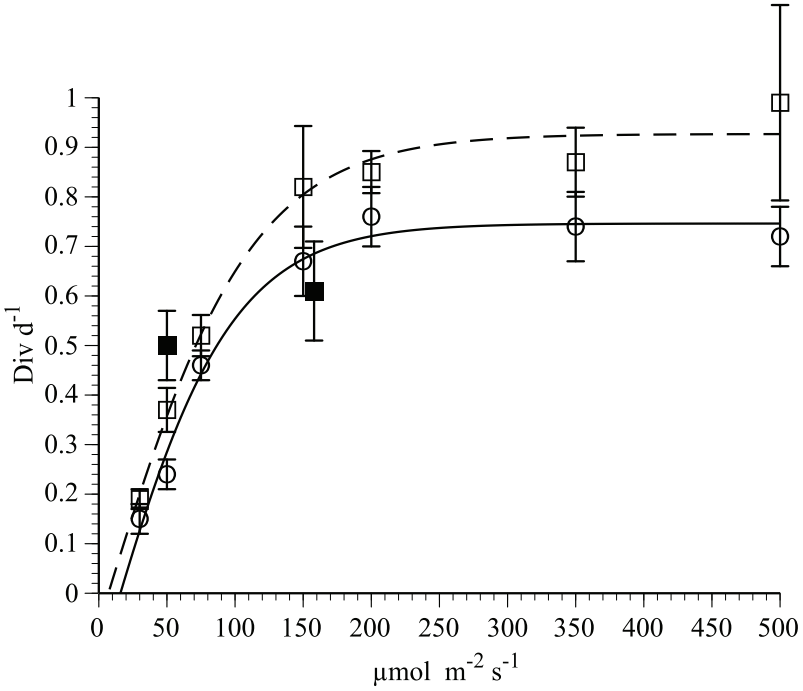

Figure 3 Irradiance-growth rate relationships for *Hemiaulus hauckii* symbiosis strains #91 and #9. Open circles and open squares are from strain #91 (7 points) in two separate experiments, solid squares (2 points) are from strain #9 measured approximately 1 year prior to strain #91. Error bars are 95% confidence intervals. Data from strain #91 are fit to a hyperbolic tangent function. Curve fit parameters are listed in Table 1 and in Article S1. Full-size DOI: 10.7717/peerj.10115/fig-3

Table 1 Results from the modified hyperbolic tangent function growth rate-irradiance and hyperbolic tangent function N_2-fixation-irradiance curve fit. The three N_2-fixation experiments were adapted to the given light levels for 7 days. The growth rate experiments were adapted at each of the light levels for 7 days. Strain 91 was used in these experiments.

Measurement	Incubation E[1]	Initial slope (α)	Realized maximum rate	E_c^1	E_k^1	R^2
N_2 fixation	50	2.079[2]	84	–	41	0.75
N_2 fixation	150	0.905[2]	155[4]	–	170	0.95
N_2 fixation	200	1.197[2]	144[4]	–	120	0.97
Growth Rate	Light gradient	0.009[3]	0.76[5]	15	84	0.99
Growth Rate	Light gradient	0.009[3]	0.93[5]	7	110	0.99

Notes:
[1] µmol m^{-2} s^{-1}.
[2] (fmol N heterocyst^{-1} h^{-1}) (µmol m^{-2} s^{-1})$^{-1}$.
[3] (div d^{-1}) (µmol m^{-2} s^{-1})$^{-1}$.
[4] (fmol N heterocyst^{-1} h^{-1}).
[5] div d^{-1}.

available N sources at approximately equal rates. The addition of ammonium in an experimental comparison resulted in higher percentages (up to 48%) of asymbiotic cells in exponential growth than when either nitrate (10–20%) was added or no N was present in the medium (10–20%) but the strain was not grown free of its symbiont (Fig. 6).

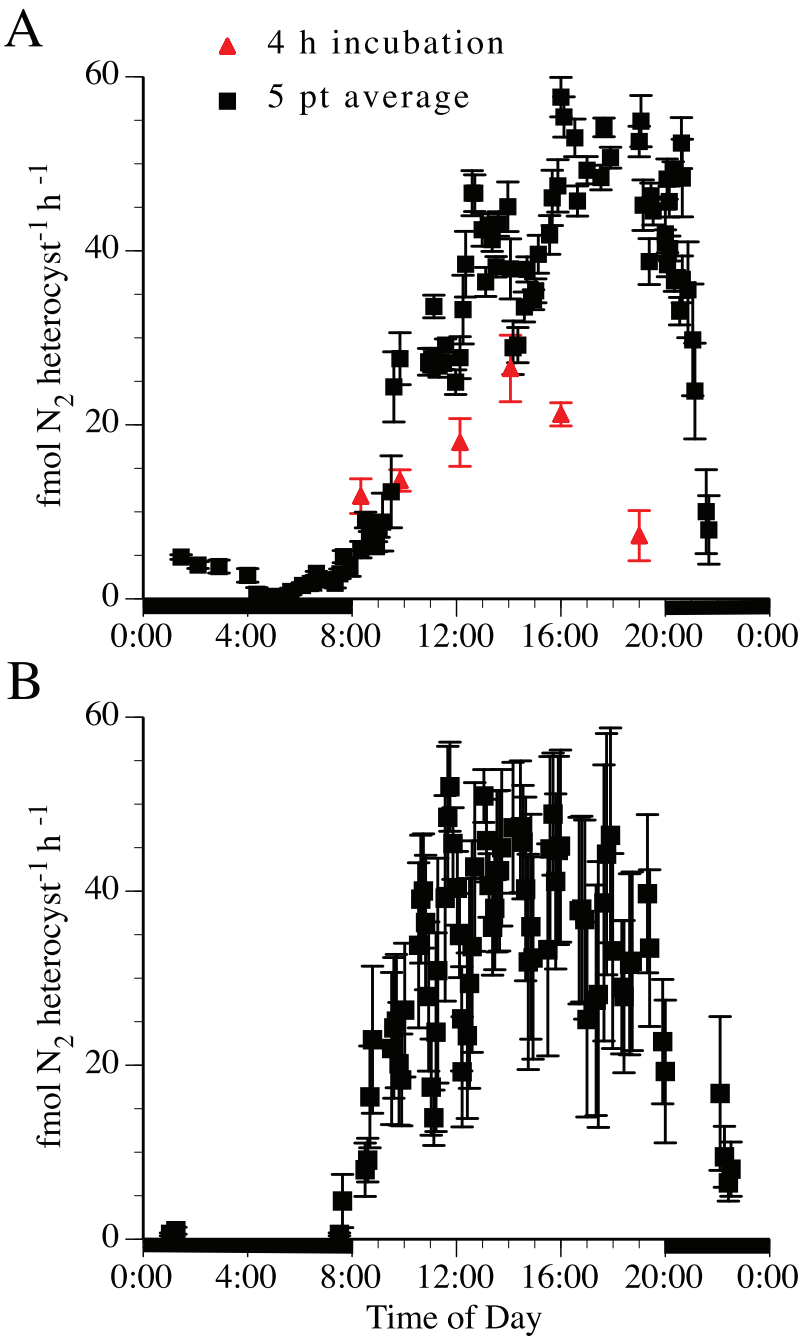

Figure 4 Diel patterns of N_2 fixation in N-free medium. (A) *Hemiaulus hauckii* symbiosis (Strain #92 = black symbols; Strain #22 = red symbol). (B) *H. membranaceus* symbiosis (Strain #82). Growth rates (*H. hauckii symbiosis*) were 0.35 ± 0.05 div d^{-1} (strain #91) and 0.43 ± 0.10 div d^{-1} (strain #22). Growth rate of the *H. membranaceus* symbiosis was 0.56 ± 0.10 div d^{-1}. Dark bars indicate nighttime. Both cultures were grown at 200 µmol m^{-2} s^{-1}. See text for details of the methodology for the 4 h and 5 pt average measurements. Error bars are standard deviation. Full-size DOI: 10.7717/peerj.10115/fig-4

A symbiont-free strain of *H. hauckii* was maintained from March 2017 to August 2017 on a solely nitrate enriched, natural seawater medium (MET-44). Ammonium concentrations in the aged stock seawater were 0.5 µm or less. When isolated and growing,

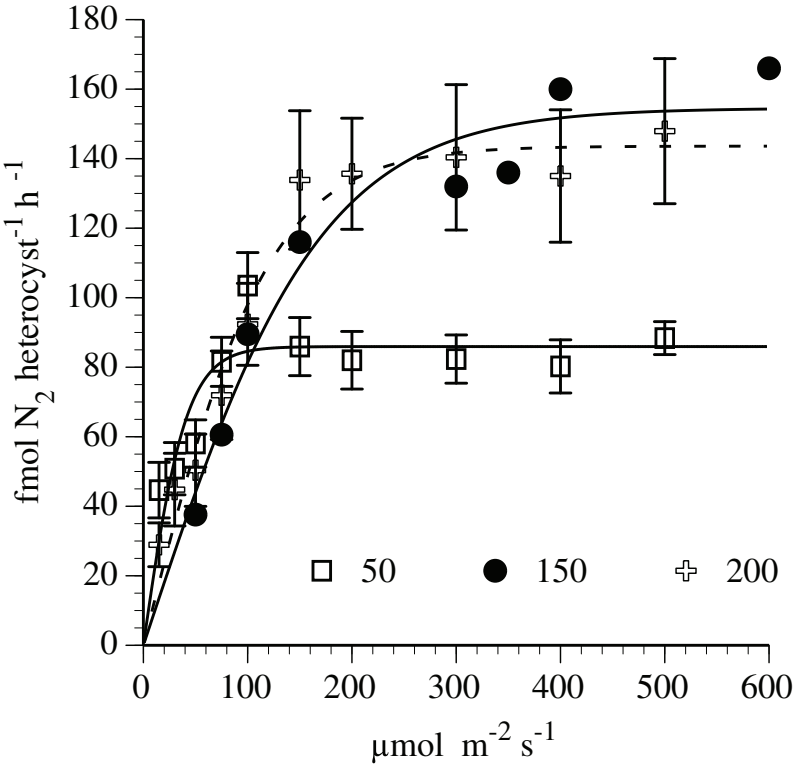

Figure 5 Irradiance-N_2 fixation rate relationships for the *Hemiaulus hauckii* symbiosis (Strain #91) adapted to three light intensities. Error bars are 95% confidence intervals.
Full-size DOI: 10.7717/peerj.10115/fig-5

it was confirmed in April 2017 to be symbiont-free by epifluorescence microscopy and maintained in a seawater-based culture medium (MET-44) that would not support the DDA strains. The strain was lost during Hurricane Harvey in August 2017 and no further information was collected.

DISCUSSION

Physiology and rate measurements of *Hemiaulus* symbioses have previously been limited to field collected and incubated samples. Using a modification of an artificial seawater medium, we have successfully and reproducibly cultured two species of *Hemiaulus* with their symbiont. *Caputo, Nylander & Foster (2019)* also reported brief success using an artificial medium; *Hilton et al. (2013)* reported genetic sequences from *Richelia* extracted from *Hemiaulus* grown using these methods.

Greatest isolation success was found when the cells were rapidly removed from the net tow cod-end, suggesting sensitivity to the various exudates found in these concentrated samples. In addition, the seawater was sterile filtered rather than autoclaved or pasteurized. Sterile filtration leaves the carbonate system and medium pH unaltered compared to heat treatment; however, viruses are not inactivated. Little is known of virus/DDA interactions, but viruses play a significant role in diatom mortality in general (*Kranzler et al., 2019*) and could be a problem for stable cultures.

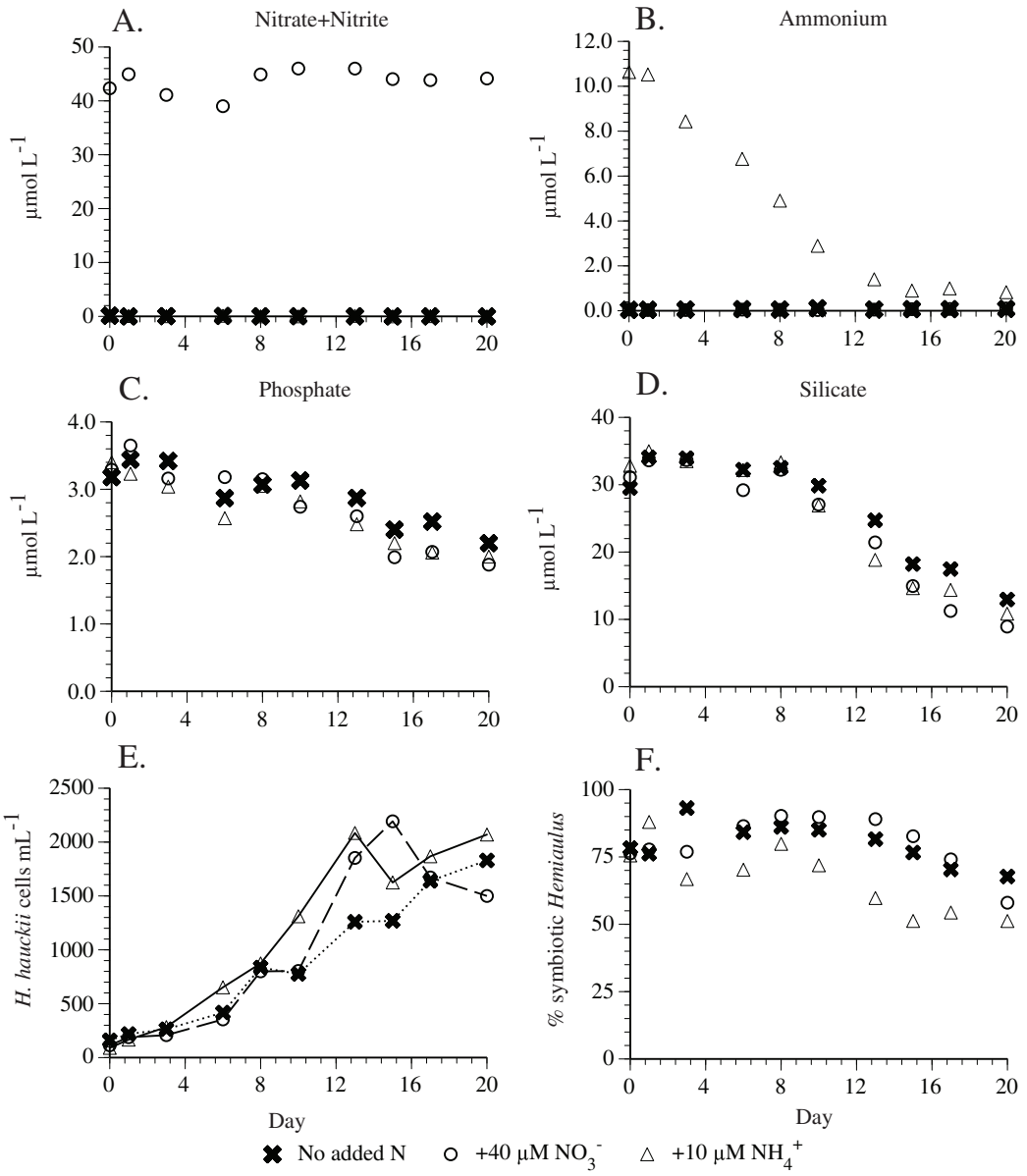

Figure 6 ***Hemiaulus hauckii*** **symbiosis growth in modified YBC-II medium under 3 nitrogen sources (N_2, nitrate, ammonium; Strain #83).** (A) Nitrate concentrations with and without added nitrate. (B) Ammonium concentrations with and without added ammonium. (C) Phosphate concentrations in the three nutrient conditions. (D) Silicate concentrations in the three nutrient conditions. (E) Cell abundance in the three nutrient conditions. (F) %*Hemiaulus* with symbionts in the three nutrient conditions. Only two symbols are visible in (A) and (B) due to overlapping near-zero values.

Full-size DOI: 10.7717/peerj.10115/fig-6

In addition, culture media designed to support phytoplankton may not support essential phycosphere components or may support difficult to remove lethal bacteria (see *Van Tol, Amin & Armbrust, 2017* for an example). The inability to culture *Hemiaulus* in a seawater-based enrichment medium used for concurrent *Rhizosolenia-Richelia* cultures suggests that the additional trace metal and chelation in our modified YBCII medium was required for sustained growth or that water quality issues are critical.

While we did not perform systematic comparisons, seawater from the Port Aransas pass is heavily influenced by both the inshore bays and coastal Gulf of Mexico. Our modified YBCII medium is free of these influences and we speculate provides a more consistent chemical environment. These difference highlights differing growth needs, sensitivities or tolerances of the *Hemiaulus* and *Rhizosolenia* DDAs that remain to be described. The oscillation between rapidly growing, apparently healthy cultures and less vigorous cultures is clearly an impediment to sustained culture as is the lack of auxospore formation. None of the isolations persisted for more than ~3 years making detailed work on model strains problematic at this time.

Previous estimates of N_2 fixation tracked ^{15}N isotope movement from the *Richelia* symbiont heterocysts to the host *Hemiaulus* cells using single-cell methods (*Foster et al., 2011*) and estimated that it was sufficient to support cell growth with a turnover time of up to 0.59 div d^{-1}. *Foster et al. (2011)* rate measurements for *H. hauckii-Richelia* (n = 17) averaged 20.4 ± 18.5 (std. dev.) fmol N heterocyst^{-1} h^{-1} (range 1.15–50.4 fmol heterocyst^{-1} h^{-1}). These heterocyst normalized rates (Foster et al.'s Table 1 footnote), are lower than the rates observed in the cultures (up to 155 fmol N_2 heterocyst^{-1} h^{-1}). Our culture growth rates (non-limiting conditions) suggest some degree of limitation in their field collections. Light/growth rate adaptation to 150–200 µmol m^{-2} s^{-1} PAR was concurrent with a maximum N_2 fixation rate approximately 6 times higher than the maximum rates observed by *Foster et al. (2011)*.

Data digitized (Plot Digitizer from SourceForge, Slashldot Media, 225 W. Broadway, Suite 1600, San Diego, CA, USA: https://sourceforge.net/) from *Carpenter et al. (1999)* Fig. 2, allows comparison of our symbiosis culture N_2 fixation rates to those from an Amazon River plume bloom where *Hemiaulus* DDA abundance reached 1.6×10^6 heterocysts L^{-1}. After extracting their N_2 fixation rates (as mg N m^{-2} d^{-1}) and concurrent heterocyst abundance from *Carpenter et al. (1999)* Fig. 2, we determined that their rates ranged from 0.6 to 40.3 fmol N heterocyst^{-1} h^{-1} and were ~8 fold lower than the maximum rates seen in cultures (note the unit conversion and comparison: mg N, fmol N or fmol N_2 fixed). These rates were generated from material collected by net and then prescreened to remove *Trichodesmium*. Based on our isolation attempts, this handling probably adversely affected the rate. *Carpenter et al. (1999)* also reported undetectable nitrate uptake in the *Hemiaulus* DDA bloom, a result consistent with our culture observations that these DDA strains did not utilize nitrate.

Many growth characteristics of *H. hauckii-R. intracellularis* are similar to the *Rhizosolenia clevei-R. intracellularis* symbiosis. Maximum growth rates are slightly less than 1 div d^{-1} and are similar between the two DDAs despite their significant size difference. Growth rates are not photoinhibited up to 500 µmol photons m^{-2} s^{-1}. Rapidly growing cells form extensive chains. Culture agitation, albeit qualitatively measured, negatively affects chain formation and possibly growth rates. The diel pattern of nitrogen fixation in the *Hemiaulus* DDA cultures parallels the diel nifH nitrogenase gene expression seen in field samples of both *Hemiaulus* DDAs (*Zehr et al., 2007*), the *Rhizosolenia* DDA (*Harke et al., 2019*) and both gene expression and acetylene reduction in the *Calothrix* symbiont of the *Chaetoceros* DDA (*Foster, Goebel & Zehr, 2010*).

The differential nitrate use by the *Hemiaulus* and *Rhizosolenia* DDAs is a significant difference between the two DDAs. Preferential NO_3^- utilization drove a higher host growth rate in a strain of the *Rhizosolenia* DDA, eventually leading to symbiont-free host cultures (*Villareal, 1990*) growing solely on NO_3^-. In field studies where N_2 appeared to be the primary N source, the *Rhizosolenia* host and symbiont DDA were tightly coupled (*Harke et al., 2019*). There are at least two mechanisms that could produce this result in the *Rhizosolenia* DDA: downregulation of symbiont diazotrophy by exposure to NO_3^- due to its extra-plasmalemma location and/or induction of host nitrate reductase pathways. The latter would result in diminished carbon flow to the symbiont in order to support nitrate assimilation into protein. Neither of these mechanisms appear to have occurred in the *H. hauckii* DDA strains we used. These results were replicated in individual experiments 4 years apart on different strains, excluding the possibility that the results were a laboratory condition artifact. For the *Hemiaulus* DDA, either nitrate cannot be used or diazotrophic supply exceeded any immediate N demand by the symbiosis and suppressed NO_3^- uptake. In contrast, ammonium was used and resulted in elevated percentages of symbiont-free hosts, but not a symbiont-free culture. The free-living marine cyanobacterium *Trichodesmium* can use NO_3^- either preferentially or concurrently during diazotrophy as an N source (*Holl & Montoya, 2005*; *Klawonn et al., 2020*; *Mulholland & Capone, 2000*) and other diazotrophs can simultaneously use N_2 and NO_3^- (*Inomura et al., 2018*). It is unusual for NO_3^- not to be used at all due to the higher overall energetic cost of nitrogen fixation added to the costs maintaining specialized cellular structures in diazotrophs (*Inomura et al., 2018*). However, in the UCYN-A/haptophyte symbiosis, the host haptophyte only assimilates diazotrophically fixed N_2 even in the presence of combined DIN (*Mills et al., 2020*). Thus, while unusual, the *H. hauckii-Richelia* symbiosis is not unique. The truly intracellular location of the *Hemiaulus* symbiont (*Caputo, Nylander & Foster, 2019*) clearly limits its contact with the environment and the potential impact of NO_3^- , but our observations also require the host *Hemiaulus* to be unresponsive to external nitrate.

In contrast, *Hemiaulus* spp. (no information on symbionts) has been reported with growth rates up to 2.2 div d^{-1} (*Furnas, 1991*) in field experiments and 3.8 div d^{-1} in nitrate-based laboratory medium (*Brand & Guillard, 1981*). While the symbiont presence is undocumented but seems unlikely given the DDA growth rates reported in our paper of <1.0 div d^{-1} as well as by modeled symbiont diazotrophy (*Inomura et al., 2020*). The *Furnas (1991)* and *Brand & Guillard (1981)* reports, as well as our briefly established asymbiotic strain on medium that would not support *Hemiaulus* DDA growth, all suggest that symbiont-free strains of *Hemiaulus* are extant in the modern ocean. *Hemiaulus* DDAs had an ancestral origin 50–100 million years ago (*Caputo, Nylander & Foster, 2019*), but asymbiotic *H. hauckii* strains apparently still persist in the modern ocean. We suggest this data supports, but does not prove, that the *Hemiaulus* DDA, with its close metabolic coupling of the host-symbiont nitrogen metabolism (*Foster & Zehr, 2019*; *Hilton et al., 2013*), is obligate and that symbiotic host *Hemiaulus* spp. are distinct from asymbiotic *Hemiaulus* strains. These asymbiotic strains should provide an invaluable tool for examining evolutionary processes in DDAs.

The growth rate and N_2 fixation results provide useful input to models examining the biogeochemical impact of the *Hemiaulus* DDA blooms in oceanic regions. The Amazon River plume is particularly noteworthy in that it has an explicit model describing the ecological-biogeochemical impacts. *Stukel et al. (2014)* model incorporated high generic N_2-based DDA growth rates >1 div d^{-1} with asymbiotic cells growing on ambient N at somewhat greater rates. Our experimental results are much lower for growth on N_2 (maximum ~0.9 div d^{-1}) and indicated no nitrate use. Non-diazotrophic, asymbiotic *Hemiaulus* growth rates from the literature are much higher than N_2-based DDA rates. These are significant alterations in the input values available to *Stukel et al. (2014)*.

In addition, our results for *H. hauckii* DDAs found no evidence of growth rate photoinhibition at the highest light level used (500 µmol m^{-2} s^{-1}). While instantaneous solar PAR may reach ~2,000 µmol m^{-2} s^{-1} (*Björkman et al., 2015*) at Station ALOHA near Hawaii (22° 45′ N 158° 00′ W), average daily PAR incident at Sta. ALOHA over the diurnal is ~850 µmol m^{-2} s^{-1} from June to August (calculated from *Letelier et al., 2017*). Vertical mixing rates will both reduce the time averaged PAR exposure exponentially with the depth of mixing as well as being rapid enough to preclude general phytoplankton photoacclimation (*Tomkins et al., 2020*). Thus, it seems possible that in-situ PAR values would not photoinhibit these DDA strains. However, damaging effects by solar UV wavelengths (*Zhu et al., 2020*) require further examination.

Follett et al. (2018) and *Inomura et al. (2020)* utilized *H. hauckii* DDA growth rates extracted from *Pyle (2011)* for modeling applications. Our report presents the full range of data in Pyle's work and notes that rates can be ~ 0.2 div d^{-1} higher than the values used by *Follett et al. (2018)* depending on the strain used. These higher rates are consistent with the mechanistic model of *Inomura et al. (2020)* in that host carbon fixation is substantial enough support to the symbiont N_2 fixation rates required for the unit DDA growth. This host derived carbon is likely to also be the reductant and energy source required to support the lengthy decline of N_2 fixation rates at the beginning of the scotophase noted in the diel experiment (Fig. 4). Further experimental verification is required.

When comparing rates, the possibility of strain-specific variation between *Foster et al. (2011)* Pacific Ocean collections, *Carpenter et al. (1999)* field collections and our Gulf of Mexico isolations cannot be excluded. Symbionts of the 3 diatom host genera have diverged with strong host specificity within diatom host genera (*Foster & Zehr, 2006*; *Janson et al., 1999*). *Bar-Zeev et al. (2008)* noted evidence of seasonally varying *Hemiaulus*-DDA dominated *Richelia* clades in the Mediterranean but there is little data to assess how physiological characteristics vary with habitat. *Rhizosolenia* and *Hemiaulus* DDA symbionts appear limited to vertical transmission during division or possibly transmission during auxosporulation (*Foster & Zehr, 2019*) raising the possibility of genetic drift of various degrees within populations (*Bar-Zeev et al., 2008*).

CONCLUSIONS

Two symbiotic associations between host diatoms and their intracellular heterocystous cyanobacterium (*Hemiaulus hauckii* - *Richelia intracellularis* and

Hemiaulus membranaceus-Richelia intracellularis) were successfully cultured for up to 3 years on artificial seawater medium. The N_2-fixation and growth rate data provided here are, to our knowledge, the first published laboratory-based data for the *Hemiaulus* DDA. This work provides details on isolation techniques that proved key to successful culturing. The symbioses are sensitive to handling, requiring rapid collection and isolation for successful growth. The cultures did not undergo sexual reproduction, and the lack of auxosporulation and concurrent size increase is a barrier to long-term stable culture. Both symbioses grow without added nitrogen other than dissolved N_2 and are supported at maximum growth rates solely by symbiont nitrogen fixation. Maximum growth rates of the intact diatom-cyanobacterium symbiosis are <1 div d^{-1} and are similar to the reported rates for another diatom-cyanobacterium symbiosis (*Rhizosolenia clevei-Richelia intracellularis*). Unlike the *Rhizosolenia clevei-Richelia intracellularis* symbiosis, the *H. hauckii – Richelia intracellularis* symbiosis does not assimilate nitrate. Nitrogen fixation by the heterocystous symbiont while within the host diatom has a clear diel pattern with maximum rates occurring during the photophase. The culture nitrogen fixation rates are consistent with field measured rates; however, maximum culture rates are ~6 to 8 times previously measured field rates. Both growth and nitrogen fixation rates follow light saturation kinetics. These data provide direct input for parameterization of light-dependent growth and nitrogen fixation in biogeochemical models.

Both literature reports and our isolation of a nitrate-utilizing, symbiont-free *Hemiaulus* culture are consistent with distinct symbiont-free and symbiont-containing lines of the diatom *Hemiaulus*. If correct, these different lineages would be useful models for understanding the evolution of these symbioses in diatoms.

ADDITIONAL INFORMATION AND DECLARATIONS

Funding

This work was supported by the National Science Foundation grants OCE 0726726 and OCE 1923667. The funders had no role in study design, data collection and analysis, decision to publish, or preparation of the manuscript.

Grant Disclosures

The following grant information was disclosed by the authors:
National Science Foundation: OCE 0726726 and OCE 1923667.

Competing Interests

Amy Pyle is employed by Blanton & Associates Inc., Austin, Texas, USA. Allison Johnson (now Allison McMillen) is employed by Park Dental Blaine, Northfield, Minnesota, USA.

Author Contributions

- Amy E. Pyle conceived and designed the experiments, performed the experiments, analyzed the data, prepared figures and/or tables, authored or reviewed drafts of the paper, and approved the final draft.

- Allison M. Johnson performed the experiments, analyzed the data, authored or reviewed drafts of the paper, and approved the final draft.
- Tracy A. Villareal conceived and designed the experiments, analyzed the data, prepared figures and/or tables, authored or reviewed drafts of the paper, and approved the final draft.

Data Availability

The following information was supplied regarding data availability:

Raw data used to create the figures and descriptive information on the curve fit selection are available as Supplemental Files.

Supplemental Information

Supplemental information for this article can be found online at http://dx.doi.org/10.7717/peerj.10115#supplemental-information.

REFERENCES

Andersen RA, Kawachi M. 2005. Chapter 6: Traditional microalgal isolation techniques. In: Andersen RA, ed. *Algal Coulture Techniques*. Burlington: Elsevier Academic Press, 83–100.

Bar-Zeev E, Yogev T, Man-Aharonovich D, Kress N, Herut B, Beja O, Berman-Frank I. 2008. Seasonal dynamics of the endosymbiotic, nitrogen-fixing cyanobacterium *Richelia intracellularis* in the eastern Mediterranean Sea. *ISME Journal* **2(9)**:911–923 DOI 10.1038/ismej.2008.56.

Brand LE, Guillard RRL. 1981. The effects of continuous light and light intensity on the reproduction rates of twenty-two species of marine phytoplankton. *Journal of Experimental Marine Biology and Ecology* **50(2–3)**:119–132 DOI 10.1016/0022-0981(81)90045-9.

Breitbarth E, Mills MM, Friedrichs G, LaRoche J. 2004. The Bunsen gas solubility coefficient of ethylene as a function of temperature and salinity and its importance for nitrogen fixation assays. *Limnology and Oceanography-Methods* **2**:282–288.

Björkman KM, Church MJ, Doggett JK, Karl DM. 2015. Differential assimilation of inorganic carbon and leucine by *Prochlorococcus* in the oligotrophic north pacific subtropical gyre. *Frontiers in Microbiology* **6(1401)**:786 DOI 10.3389/fmicb.2015.01401.

Brzezinski MA, Villareal TA, Lipschultz F. 1998. Silica production and the contribution of diatoms to new and primary production in the central North Pacific. *Marine Ecology Progress Series* **167**:89–104 DOI 10.3354/meps167089.

Campbell L, Olson RJ, Sosik HM, Abraham A, Henrichs DW, Hyatt CJ, Buskey EJ. 2010. First harmful *Dinophysis* (Dinophyceae, Dinophyceales) bloom in the U.S. is revealed by automated imaging flow cytometry. *Journal of Phycology* **46(1)**:66–75 DOI 10.1111/j.1529-8817.2009.00791.x.

Campbell L, Henrichs DW, Peacock EE, Futrelle J, Sosik HM. 2017. Imaging FlowCytobot provides novel insights on phytoplankton community dynamics. In: Proenca LAO, Hallegraeff G, eds. *Proceedings of the 17th International Conference on Harmful Algae. International Society for the Study of Harmful Algae and Intergovernmental Oceanographic Commission of UNESCO 2017*.

Capone DG. 1993. Determination of nitrogenase activity in aquatic samples using the acetylene reduction procedure. In: Kemp PF, Sherr BF, Sherr EB, Cole JJ, eds. *Handbook of Methods in Aquatic Microbial Ecology*. New York: Lewis Publishers, 621–631.

Caputo A, Nylander JAA, Foster RA. 2019. The genetic diversity and evolution of diatom-diazotroph associations highlights traits favoring symbiont integration. *FEMS Microbiology Letters* **366(2)**:fny297 DOI 10.1093/femsle/fny297.

Carpenter EJ. 2002. Marine cyanobacterial symbioses. *Biology and Environment* **102B(1)**:15–18 DOI 10.3318/bioe.2002.102.1.15.

Carpenter EJ, Janson S. 2000. Intracellular cyanobacterial symbionts in the marine diatom *Climacodium frauenfeldianum* (Bacillariophyceae). *Journal of Phycology* **36(3)**:540–544 DOI 10.1046/j.1529-8817.2000.99163.x.

Carpenter EJ, Montoya JP, Burns J, Mulholland MR, Subramaniam A, Capone DG. 1999. Extensive bloom of a N_2-fixing diatom/cyanobacterial association in the tropical Atlantic Ocean. *Marine Ecology-Progress Series* **185**:273–283 DOI 10.3354/meps185273.

Chen YB, Zehr JP, Mellon M. 1996. Growth and nitrogen fixation of the diazotrophic filamentous nonheterocystous cyanobacterium *Trichodesmium* sp. IMS 101 in defined media: Evidence for a circadian rhythm. *Journal of Phycology* **32**:916–923.

Cooley SR, Coles VJ, Subramaniam A, Yager PL. 2007. Seasonal variations in the Amazon plume-related atmospheric carbon sink. *Global Biogeochemical Cycles* **21(3)**:002831 DOI 10.1029/2006GB002831.

Dore JE, Letelier RM, Church MJ, Lukas R, Karl DM. 2008. Summer phytoplankton blooms in the oligotrophic North Pacific subtropical gyre: historical perspective and recent observations. *Progress in Oceanography* **76(1)**:2–38 DOI 10.1016/j.pocean.2007.10.002.

Eppley RW, Peterson BJ. 1979. Particulate organic matter flux and planktonic new production in the deep ocean. *Nature* **282(5740)**:677–680 DOI 10.1038/282677a0.

Farnelid H, Turk-Kubo K, Ploug H, Ossolinski JE, Collins JR, Van Mooy BAS, Zehr JP. 2019. Diverse diazotrophs are present on sinking particles in the North Pacific Subtropical Gyre. *ISME Journal* **13(1)**:170–182 DOI 10.1038/s41396-018-0259-x.

Follett CL, Dutkiewicz S, Karl DM, Inomura K, Follows MJ. 2018. Seasonal resource conditions favor a summertime increase in North Pacific diatom-diazotroph associations. *ISME Journal* **12(6)**:1543–1557 DOI 10.1038/s41396-017-0012-x.

Fong AA, Karl DM, Lukas R, Letelier RM, Zehr JP, Church MJ. 2008. Nitrogen fixation in an anticyclonic eddy in the oligotrophic North Pacific Ocean. *ISME Journal* **2(6)**:663–676 DOI 10.1038/ismej.2008.22.

Foster RA, Carpenter EJ, Bergman B. 2006. Unicellular cyanobionts in open ocean dinoflagellates, radiolarians, and tintinnids: ultrastructural characterization and immuno-localization of phycoerythrin and nitrogenase. *Journal of Phycology* **42(2)**:453–463 DOI 10.1111/j.1529-8817.2006.00206.x.

Foster RA, Goebel NL, Zehr JP. 2010. Isolation of *Calothrix rhizosoleniae* (Cyanobacteria) strain SC01 from *Chaetoceros* (Bacillariophyta) spp. diatoms of the subtropical North Pacific Ocean. *Journal of Phycology* **46(5)**:1028–1037 DOI 10.1111/j.1529-8817.2010.00885.x.

Foster RA, Kuypers MMM, Vagner T, Paerl RW, Musat N, Zehr JP. 2011. Nitrogen fixation and transfer in open ocean diatom-cyanobacterial symbioses. *ISME Journal* **5(9)**:1484–1493 DOI 10.1038/ismej.2011.26.

Foster RA, O'Mullan GD. 2008. Nitrogen-fixing and nitrifying symbioses in the marine environment. In: Capone DG, Bronk DA, Mulholland MR, Carpenter EJ, eds. *Nitrogen in the Marine Environment*. Second Edition. San Diego: Elsevier, 1197–1218.

Foster RA, Subramaniam A, Mahaffey C, Carpenter EJ, Capone DG, Zehr JP. 2007. Influence of the Amazon River plume on distributions of free-living and symbiotic cyanobacteria in the

western tropical north Atlantic Ocean. *Limnology and Oceanography* **52(2)**:517–532 DOI 10.4319/lo.2007.52.2.0517.

Foster RA, Subramaniam A, Zehr JP. 2009. Distribution and activity of diazotrophs in the Eastern Equatorial Atlantic. *Environmental Microbiology* **11(4)**:741–750 DOI 10.1111/j.1462-2920.2008.01796.x.

Foster RA, Zehr JP. 2006. Characterization of diatom-cyanobacteria symbioses on the basis of nifH, hetR and 16S rRNA sequences. *Environmental Microbiology* **8(11)**:1913–1925 DOI 10.1111/j.1462-2920.2006.01068.x.

Foster RA, Zehr JP. 2019. Diversity, genomics, and distribution of phytoplankton-cyanobacterium single-cell symbiotic associations. *Annual Review of Microbiology* **73(1)**:435–456 DOI 10.1146/annurev-micro-090817-062650.

Furnas MJ. 1991. Net in situ growth rates of phytoplankton in an oligotrophic, tropical shelf ecosystem. *Limnology and Oceanography* **36(1)**:13–29 DOI 10.4319/lo.1991.36.1.0013.

Grasshoff KK, Kremling K, Ehrhardt M. 1999. *Methods of seawater analysis*. Weinheim: Wiley-VCH, 599.

Grosse J, Bombar D, Hai ND, Lam NN, Voss M. 2009. The Mekong River plume fuels nitrogen fixation and determines phytoplankton species distribution in the South China Sea during low- and high-discharge season. *Limnology and Oceanography* **55(4)**:1668–1680 DOI 10.4319/lo.2010.55.4.1668.

Guillard RRL. 1973. Division rates. In: Stein JR, ed. *Handbook of Phycological Methods Culture Methods and Growth Measurements*. New York: Cambridge University Press, 290–320.

Guillard RRL, Hargraves PE. 1993. *Stichochrysis immobilis* is a diatom, not a chrysopyte. *Phycologia* **32**:234–236.

Hallegraeff GM, Jeffrey SW. 1984. Tropical phytoplankton species and pigments of continental shelf waters of North and North-west Australia. *Marine Ecology-Progress Series* **20**:59–74 DOI 10.3354/meps020059.

Harding K, Turk-Kubo KA, Sipler RE, Mills MM, Bronk DA, Zehr JP. 2018. Symbiotic unicellular cyanobacteria fix nitrogen in the Arctic Ocean. *Proceedings of the National Academy of Sciences of the United States of America* **115(52)**:13371–13375 DOI 10.1073/pnas.1813658115.

Harke MJ, Frischkorn KR, Haley ST, Aylward FO, Zehr JP, Dyhrman ST. 2019. Periodic and coordinated gene expression between a diazotroph and its diatom host. *ISME Journal* **13(1)**:118–131 DOI 10.1038/s41396-018-0262-2.

Heinbokel JF. 1986. Occurrence of *Richelia intracellularis* (Cyanophyta) within the diatoms *Hemiaulus hauckii* and H. membranaceus off Hawaii. *Journal of Phycology* **22(3)**:399–403 DOI 10.1111/j.1529-8817.1986.tb00043.x.

Hilton JA, Foster RA, Tripp HJ, Carter BJ, Zehr JP, Villareal TA. 2013. Genomic deletions disrupt nitrogen metabolism pathways of a cyanobacterial diatom symbiont. *Nature Communications* **4(1)**:1767 DOI 10.1038/ncomms2748.

Holl CM, Montoya JP. 2005. Interactions between nitrate uptake and nitrogen fixation in continuous cultures of the marine diazotroph *Trichodesmium* (Cyanobacteria). *Journal of Phycology* **41(6)**:1178–1183 DOI 10.1111/j.1529-8817.2005.00146.x.

Inomura K, Bragg J, Riemann L, Follows MJ. 2018. A quantitative model of nitrogen fixation in the presence of ammonium. *PLOS ONE* **13(11)**:e0208282 DOI 10.1371/journal.pone.0208282.

Inomura K, Follett CL, Masuda T, Eichner M, Prasil O, Deutsch C. 2020. Carbon transfer from the host diatom enables fast growth and high rate of N_2 fixation by symbiotic heterocystous cyanobacteria. *Plants-Basel* **9(2)**:16 DOI 10.3390/plants9020192.

Janson S, Wouters J, Bergman B, Carpenter EJ. 1999. Host specificity in the *Richelia*—diatom symbiosis revealed by hetR gene sequence analysis. *Environmental Microbiology* **1(5)**:431–438 DOI 10.1046/j.1462-2920.1999.00053.x.

Jassby AD, Platt T. 1976. Mathematical formulation of the relationship between photosynthesis and light for phytoplankton. *Limnology and Oceanography* **21**:540–547.

Jensen BB, Cox RP. 1983. Direct measurements of steady-state kinetics of cyanobacterial N_2 uptake by membrane-leak mass spectrometry and comparisons between nitrogen fixation and acetylene reduction. *Applied and Environmental Microbiology* **45**:1331–1337 DOI 10.1128/aem.45.4.1331-1337.1983.

Karl DM, Church MJ, Dore JE, Letelier RM, Mahaffey C. 2012. Predictable and efficient carbon sequestration in the North Pacific Ocean supported by symbiotic nitrogen fixation. *Proceedings of the National Academy of Sciences of the United States of America* **109(6)**:1842–1849 DOI 10.1073/pnas.1120312109.

Karsten G. 1905. Das phytoplankton des Atlantischen Ozeans nach dem material der deutschen Tiefsee-Expedition 1898–1899. *Wissen Erg Deut Tiefsee-Exped "VALDIVA"* **2**:137–219.

Kimor B, Reid FMH, Jordan JB. 1978. An unusual occurrence of *Hemiaulus membranaceus* Cleve (Bacillariophyceae) with *Richelia intracellularis* Schmidt (Cyanophyceae) off the coast of Southern California in October 1976. *Phycologia* **17**:162–166.

Klawonn I, Eichner MJ, Wilson ST, Moradi N, Thamdrup B, Kümmel S, Gehre M, Khalili A, Grossart H-P, Karl DM, Ploug H. 2020. Distinct nitrogen cycling and steep chemical gradients in *Trichodesmium* colonies. *ISME Journal* **14(2)**:399–412 DOI 10.1038/s41396-019-0514-9.

Kranzler CF, Krause JW, Brzezinski MA, Edwards BR, Biggs WP, Maniscalco M, McCrow JP, Van Mooy BAS, Bidle KD, Allen AE, Thamatrakoln K. 2019. Silicon limitation facilitates virus infection and mortality of marine diatoms. *Nature Microbiology* **4(11)**:1790–1797 DOI 10.1038/s41564-019-0502-x.

Letelier RM, White AE, Bidigare RR, Barone B, Church MJ, Karl DM. 2017. Light absorption by phytoplankton in the North Pacific Subtropical Gyre. *Limnology and Oceanography* **62**:1526–1540 DOI 10.1002/lno.10515.

Mills MM, Turk-Kubo KA, Van Dijken GL, Henke BA, Harding K, Wilson ST, Arrigo KR, Zehr JP. 2020. Unusual marine cyanobacteria/haptophyte symbiosis relies on N2 fixation even in N-rich environments. *ISME Journal* **14**:2395–2406 DOI 10.1038/s41396-020-0691-6.

Mulholland MR, Capone DG. 2000. The nitrogen physiology of the marine N_2-fixing cyanobacteria *Trichodesmium* spp. *Trends in Plant Science* **5(4)**:148–153 DOI 10.1016/S1360-1385(00)01576-4.

Ohki K, Zehr JP, Fujita Y. 1992. Trichodesmium-establishment of culture and characteristics of N_2 fixation. In: Carpenter EJ, Capone DG, Reuter JG, eds. *Marine Pelagic Cyanobacteria : Trichodesmium and Other Diazotrophs*. Alphen aan den Rijn: Kluwer, 307–318.

Pyle A. 2011. Light dependant growth and nitrogen fixation rates in the *Hemiaulus hauckii* and *Hemiaulus membranaceus* diatom-diazotroph associations. M.S. thesis. The University of Texas at Austin, 77.

Scharek R, Latasa M, Karl DM, Bidigare RR. 1999. Temporal variations in diatom abundance and downward vertical flux in the oligotrophic North Pacific gyre. *Deep-Sea Research Part I-Oceanographic Research Papers* **46(6)**:1051–1075 DOI 10.1016/S0967-0637(98)00102-2.

Schouten S, Villareal T, Hopmans E, Mets A, Swanson K, Damste J. 2013. Endosymbiotic heterocystous cyanobacteria synthesize different heterocyst glycolipids than free-living heterocystous cyanobacteria. *Phytochemistry* **85**:115–121 DOI 10.1016/j.phytochem.2012.09.002.

Schöne HK, Schöne A. 1982. MET 44: a weakly enriched sea-water medium for ecological sudies on marine plankton algae, and some examples of its application. *Botanica Marina* **25**:117–122.

Stukel MR, Coles VJ, Brooks MT, Hood RR. 2014. Top-down, bottom-up and physical controls on diatom-diazotroph assemblage growth in the Amazon River plume. *Biogeosciences* **11(12)**:3259–3278 DOI 10.5194/bg-11-3259-2014.

Subramaniam A, Yager PL, Carpenter EJ, Mahaffey C, Bjorkman K, Cooley S, Kustka AB, Montoya JP, Sanudo-Wilhelmy SA, Shipe R, Capone DG. 2008. Amazon River enhances diazotrophy and carbon sequestration in the tropical North Atlantic Ocean. *Proceedings of the National Academy of Sciences of the United States of America* **105(30)**:10460–10465 DOI 10.1073/pnas.0710279105.

Taylor FJR. 1982. Symbioses in marine microplankton. *Annales de l'Institut Océanographique* **S58**:61–90.

Tomkins M, Martin AP, Nurser AJG, Anderson TR. 2020. Phytoplankton acclimation to changing light intensity in a turbulent mixed layer: a Lagrangian modelling study. *Ecological Modelling* **417**:108917 DOI 10.1016/j.ecolmodel.2019.108917.

Van Tol HM, Amin SA, Armbrust EV. 2017. Ubiquitous marine bacterium inhibits diatom cell division. *ISME Journal* **11(1)**:31–42 DOI 10.1038/ismej.2016.112.

Venrick EL. 1974. The distribution and significance of *Richelia intracellularis* Schmidt in the North Pacific Central Gyre. *Limnology and Oceanography* **19(3)**:437–445 DOI 10.4319/lo.1974.19.3.0437.

Villareal TA. 1989. Division cycles in the nitrogen-fixing *Rhizosolenia* (Bacillariophyceae)-*Richelia* (Nostocaceae) symbiosis. *British Phycological Journal* **24(4)**:357–365 DOI 10.1080/00071618900650371.

Villareal TA. 1990. Laboratory cultivation and preliminary characterization of the *Rhizosolenia* (Bacillariophyceae)-*Richelia* (Cyanophyceae) symbiosis. *Marine Ecology* **11(2)**:117–132 DOI 10.1111/j.1439-0485.1990.tb00233.x.

Villareal TA. 1991. Nitrogen fixation by the cyanobacterial symbiont of the diatom genus *Hemiaulus*. *Marine Ecology Progress Series* **76**:201–204 DOI 10.3354/meps076201.

Villareal TA. 1992. Marine nitrogen-fixing diatom-cyanobacterial symbioses. In: Carpenter EJ, Capone DG, Reuter J, eds. *Marine Pelagic Cyanobacteria: Trichodesmium and other Diazotrophs*. Netherlands: Kluwer, 163–175.

Villareal TA. 1994. Widespread occurrence of the *Hemiaulus*-cyanobacterial symbiosis in the Southwest North Atlantic Ocean. *Bulletin of Marine Science* **53**:1–7.

Villareal TA, Adornato L, Wilson C, Shoenbachler CA. 2011. Summer blooms of diatom-diazotroph assemblages (DDAs) and surface chlorophyll in the N. Pacific gyre—a disconnect. *Journal of Geophysical Research-Oceans* **116(C3)**:e6268 DOI 10.1029/2010JC006268.

Villareal TA, Brown CG, Brzezinski MA, Krause JW, Wilson C. 2012. Summer diatom blooms in the North Pacific subtropical gyre: 2008–2009. *PLOS ONE* **7(4)**:e33109 DOI 10.1371/journal.pone.0033109.

Weber SC, Carpenter EJ, Coles VJ, Yager PL, Goes J, Montoya JP. 2017. Amazon River influence on nitrogen fixation and export production in the western tropical North Atlantic. *Limnology and Oceanography* **62(2)**:618–631 DOI 10.1002/lno.10448.

Welschmeyer NA. 1994. Fluorometric analysis of chlorophyll a in the presence of chlorophyll b and pheopigments. *Limnology and Oceanography* **39(8)**:1985–1992 DOI 10.4319/lo.1994.39.8.1985.

White AE, Spitz YH, Letelier RM. 2007. What factors are driving summer phytoplankton blooms in the North Pacific Subtropical Gyre? *Journal of Geophysical Research-Oceans* **112(C12)**:779 DOI 10.1029/2007JC004129.

Wilson C, Villareal TA, Bogard SJ. 2004. Large-scale forcing of late summer chlorophyll blooms in the oligotrophic Pacific. In: *AGU Winter meeting, 13–17 December 2005, San Francisco, CA*.

Wilson C, Villareal TA, Maximenko N, Montoya JP, Bograd SJ, Schoenbaechler CA. 2008. Biological and physical forcings of late summer chlorophyll blooms at 30° N in the oligotrophic Pacific. *Journal of Marine Systems* **69(3–4)**:164–176 DOI 10.1016/j.jmarsys.2005.09.018.

Yeung LY, Berelson WM, Young ED, Prokopenko MG, Rollins N, Coles VJ, Montoya JP, Carpenter EJ, Steinberg DK, Foster RA, Capone DG, Yager PL. 2012. Impact of diatom-diazotroph associations on carbon export in the Amazon River plume. *Geophysical Research Letters* **39(18)**:L18609 DOI 10.1029/2012GL053356.

Zehr JP, Montoya JP, Jenkins BD, Hewson I, Mondragon E, Short CM, Church MJ, Hansen A, Karl DM. 2007. Experiments linking nitrogenase gene expression to nitrogen fixation in the North Pacific subtropical gyre. *Limnology and Oceanography* **52(1)**:169–183 DOI 10.4319/lo.2007.52.1.0169.

Zehr JP, Capone DG. 2020. Changing perspectives in marine nitrogen fixation. *Science* **368(6492)**:729 DOI 10.1126/science.aay9514.

Zehr JP. 2011. Nitrogen fixation by marine cyanobacteria. *Trends in Microbiology* **19(4)**:162–173 DOI 10.1016/j.tim.2010.12.004.

Zhu Z, Fu FX, Qu PP, Mak EWK, Jiang HB, Zhang RF, Zhu ZY, Gao KS, Hutchins DA. 2020. Interactions between ultraviolet radiation exposure and phosphorus limitation in the marine nitrogen-fixing cyanobacteria *Trichodesmium* and *Crocosphaera*. *Limnology and Oceanography* **65(2)**:363–376 DOI 10.1002/lno.11304.